Molecular Crystals and Liquid Crystals
Publication details, including instructions for authors and subscription information:
http://www.tandfonline.com/loi/gmcl16

Dilatation and Dielectric Anomalies in Single Crystal Phenanthrene

Donald A. Miller [a c], J. W. Kauffman [a], C. R. Kannewurf [a] & R. A. Arndt [b]
[a] Technological Institute Northwestern University, Evanston, Ill, 60201
[b] COMSAT Laboratories, Clarksburg, Maryland, 20734
[c] IBM Corporation, Essex Junction, Vermont, 05452
Version of record first published: 26 Apr 2007.

To cite this article: Donald A. Miller , J. W. Kauffman , C. R. Kannewurf & R. A. Arndt (1972): Dilatation and Dielectric Anomalies in Single Crystal Phenanthrene, Molecular Crystals and Liquid Crystals, 15:4, 329-345

To link to this article: http://dx.doi.org/10.1080/15421407208083569

Molecular Crystals and Liquid Crystals. 1972. Vol. 15, pp. 329–345

Printed in Great Britain

Dilatation and Dielectric Anomalies in Single Crystal Phenanthrene†‡

DONALD A. MILLER,§ J. W. KAUFFMAN and C. R. KANNEWURF

Technological Institute
Northwestern University
Evanston, Ill. 60201

and

R. A. ARNDT

COMSAT Laboratories
Clarksburg, Maryland, 20734

Received August 31, 1970; *in revised form April* 15, 1971

Abstract—Capacitance data on single crystal phenanthrene have been obtained from 25 to 75 °C using a capacitance bridge capable of resolving changes on the order 10^{-5} pF. The measured capacitance has been found to depend on frequency, temperature, rates of temperature change, and on the thermal history of the specimen. A specially designed capacitance-type dilatometer has been employed to observe length changes on the order of 100 Å in 5 mm specimens over the temperature range of 24 to 82 °C. In the vicinity of 73 °C, the thermal expansion coefficient peaks sharply along the direction of the a and c' axes of the monoclinic structure and dips sharply along the direction of the b axis, the two-fold symmetry axis. The dielectric permittivity was measured in the c' direction and correlated with dilatation results.

1. Introduction

Recent literature on phenanthrene has reported anomalous phenomena which were unexpected from knowledge on anthracene, its structural isomer. These have included anomalies in resistivity and heat capacity, as well as electrical polarization phenomena. All of these phenomena are associated with a critical temperature in the vicinity of 68 to 72 °C; no polymorphic phase transformations in the

† This research was supported in part by the Advanced Research Projects Agency of the Department of Defense through the Northwestern University Materials Research Center.

‡ Work performed while one of us (R. A. A.) was at Brookhaven National Laboratory, Upton, Long Island, New York.

§ Present address: IBM Corporation, Essex Junction, Vermont 05452.

same temperature range have been found with which to identify these phenomena. Improvements in purification processes have shown the phenomena to be intrinsic to phenanthrene in the solid state.[1–11]

As an aid to understanding these phenomena, the present investigation presents the results of high resolution dielectric studies on single crystal phenanthrene. For use in analyzing the dielectric data, high resolution dilatometry studies were also undertaken. The present work reports previously unpublished peaks for the thermal expansion coefficients in the a and c' directions of the monoclinic lattice and a dip in the direction of b, the two-fold symmetry axis, all of which occur in the vicinity of 73.3 °C. The dielectric data, which have only been obtained along the c' direction, show a dependence on frequency, temperature, rates of temperature change, and on the thermal history of the specimen. Of these variables, all but the first also influence the dilatometry results.

2. Dielectric Measurements

As can readily be demonstrated by a simple capacitance calculation, small dimensions of a planar dielectric specimen may prevent the practical use of guard ring electrodes on the specimen.

The mechanical and chemical properties of phenanthrene prevent the use of high contact pressure and many conductive preparations for obtaining electrode contacts with no air gaps. The most satisfactory electrodes were prepared by the use of several colloidal graphite preparations. Two pieces of brass shim stock, in which 0.635 cm i.d. holes had been punched, were precisely aligned with respect to each other by means of steel pins. A specimen could be held between these pieces without damage. A very light coat of a graphite–alcohol aerosol was then sprayed through each mask from a maximum distance possible and permitted to dry. This procedure was used to keep as much organic solvent off the sample as possible and repeated until an opaque layer was obtained. The shielded specimen chamber contained a fixed metal electrode to which the specimen could be mechanically and electrically connected by means of a graphite-in-water suspension. A coaxial lead was then connected to the upper surface of the specimen by means of the same colloidal

graphite preparation. After several hours of air drying, to permit escape of water vapor from the electrode materials, the test chamber and associated components were placed in a glove bag of argon, which was then flushed and refilled several times. The chamber would be permitted to stand overnight, then sealed and removed from the glove bag.

The typical specimen for which data are reported here was a cleavage plate of phenanthrene which had well-defined surfaces and a thickness of 0.4175 mm. Light polishing was performed on lens tissue over a plate-glass surface, dampened with ethanol. After thorough air drying, colloidal graphite electrodes were deposited through masks, as previously described, and the specimen was mounted in the test chamber. The electrodes did not extend to the irregularly shaped edges of the specimen. The capacitor electrodes were thus maintained parallel to the crystal surfaces with essentially negligible pressure and no air gaps. Microscopic examination of all specimens revealed no evidence of sublimation from under the electrodes. Since the electrodes firmly adhered to the specimen, the dimensional variation of the specimen with temperature should influence the measured capacitance only through the specimen thickness.

The appearance of some unusual behavior in the dielectric properties was briefly discussed in a preliminary report.[11] Figure 1 shows data obtained for a 5 kHz excitation. Two qualitatively different types of behavior were found, depending on the rate of temperature change. Starting at the top of the graph, the first three symbols □, △ and ◇ represent changes of a few tenths degree per minute. On the first heating cycle, represented by the symbol □, the curve leveled off near 65 °C, increased to a peak around 69 °C, then decreased steeply. As represented by the symbol △, cooling at the same rate produced no evidence of a peak down to 62 °C. The two triangles at 62° show the drift occurring during a 15-hour interval. The symbol ◇ shows that, on reheating at the same rate, the capacitance followed a constant slope up to 69°, where it fluctuated strongly. After being monitored for 281 minutes, the capacitance was observed to stabilize at a low value. Upon heating above 69 °C, the capacitance decreased at a steeper slope. This behavior suggests that cooling at several tenths degree per

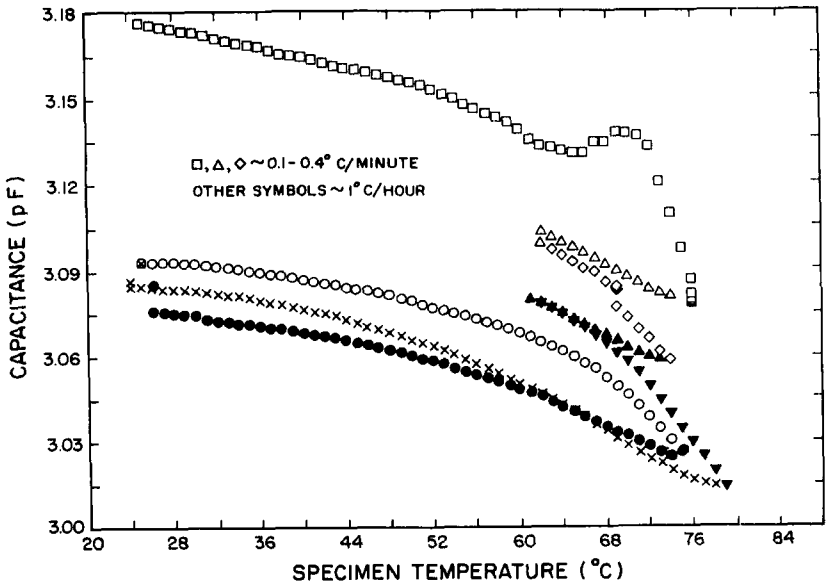

Figure 1. Dielectric capacitance along the c' direction at an excitation frequency of 5 kHz on a single crystal sample.

minute caused the specimen to be " quenched ", or frozen into the higher temperature form. As represented by the symbols ▲, ▼ and ×, a smoother variation was observed at changes of 1 °C/hour for both heating and cooling. An overall discrepancy is seen between the initial and final room temperature values. However, a partial recovery is seen to have occurred during a 38-day pause at room temperature.

Superimposed on the first set of data is the 5 kHz portion of the data from a subsequent run which was made at changes of 1 °C/hour. The symbols ○ and ● represent heating and cooling, respectively. Note the apparent hysteresis, with partial recovery occurring during a 15-day pause at room temperature.

The edge and vacuum capacitances, C_E and C_V respectively, were calculated for arbitrary choices of κ_R, the relative dielectric constant. The last three columns of Table 1 show the results of calculating κ_R for each of three values selected from the capacitance data. These values were selected from the 26 °C data of Fig. 1: at the start of the first run, and at the start and end of the second run, prior to

the 15-day pause. Comparison with the first column shows that self consistency in the calculations is obtained for $\kappa_R \simeq 4.15 \pm 0.07$ (see the three italicised values in Table 1). This value is higher than that expected from earlier work.[8] However, it should be remembered that the previously reported value of 3.0 ± 0.2 resolved no changes with either temperature or frequency, and the present work found a definite dependence on both parameters. Furthermore, the

TABLE 1 Values of the Relative Dielectric Constant Obtained in the Self-consistent Procedure for Identifying κ_R from the data at 26 °C

κ_R	C_E(pF)	$(3.175 - C_E)/C_V$	$(3.093 - C_E)/C_V$	$(3.075 - C_E)/C_V$
2.6	0.27808	4.313	4.191	4.164
2.7	0.28187	4.308	4.186	4.159
2.8	0.28566	4.302	4.180	4.153
2.9	0.28945	4.296	4.174	4.148
3.0	0.29325	4.291	4.167	4.142
3.1	0.29704	4.285	4.163	4.136
3.2	0.30083	4.279	4.157	4.130
3.3	0.30462	4.274	4.152	4.125
3.4	0.30841	4.268	4.146	4.119
3.5	0.31220	4.262	4.140	4.114
3.6	0.31599	4.257	4.125	4.108
3.7	0.31978	4.251	4.129	4.102
3.8	0.32357	4.246	4.124	4.097
3.9	0.32736	4.240	4.118	4.091
4.0	0.33115	4.224	4.112	4.085
4.1	0.33494	4.229	*4.106*	*4.080*
4.2	0.33873	*4.223*	4.101	4.074
4.3	0.34252	4.217	4.095	4.068
4.4	0.34631	4.212	4.090	4.063
4.5	0.35010	4.206	4.084	4.057

Thus: $\kappa_R \simeq 4.15 \pm 0.07$

previous work employed spring loaded plates for the electrodes. It is not surprising that the relative dielectric constants of this and the previous work are larger than the values reported for compressed powder specimens.[12]

Figure 2 shows the superposition of capacitance versus temperature curves for seven frequencies. The upper and lower curve segments for each symbol represent heating and cooling respectively. The

recovery value at each frequency for the fifteen-day pause at room temperature is the final point on the cooling segment. Figure 3 shows values selected from the data of Fig. 2 replotted against frequency for various temperatures: at every 10 degrees on heating from 25 to 75 °C, and at values offset 1 °C on cooling. The symbols △ and ○ represent heating and cooling, respectively. The 15-day recovery values are represented by the symbol ●. Measurements

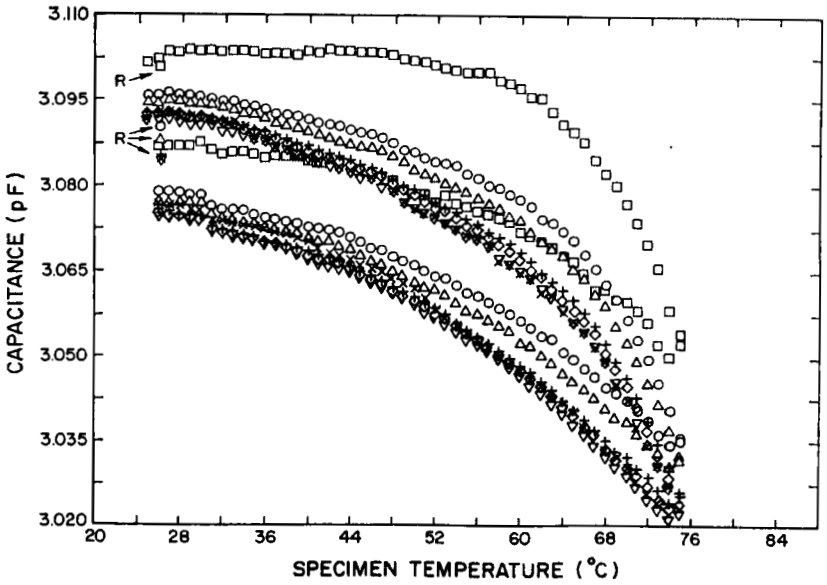

Figure 2. Dielectric capacitance at seven different excitation frequencies. The symbols □, ○, △, +, ◇, ▽, and × represent 0.1, 0.5, 1, 5, 10, 50 and 100 kHz respectively. The various R points represent the final fifteen-day recovery values for each frequency.

could only be made down to 100 Hz. As would be even more apparent with a linear frequency scale, the major capacitance variation is in the low frequency region, with only minor changes above 10 kHz. This is consistent with the so-called interfacial polarization described in the literature for dielectrics.[13] The dissipation factor was always too small to measure on the capacitance bridge.

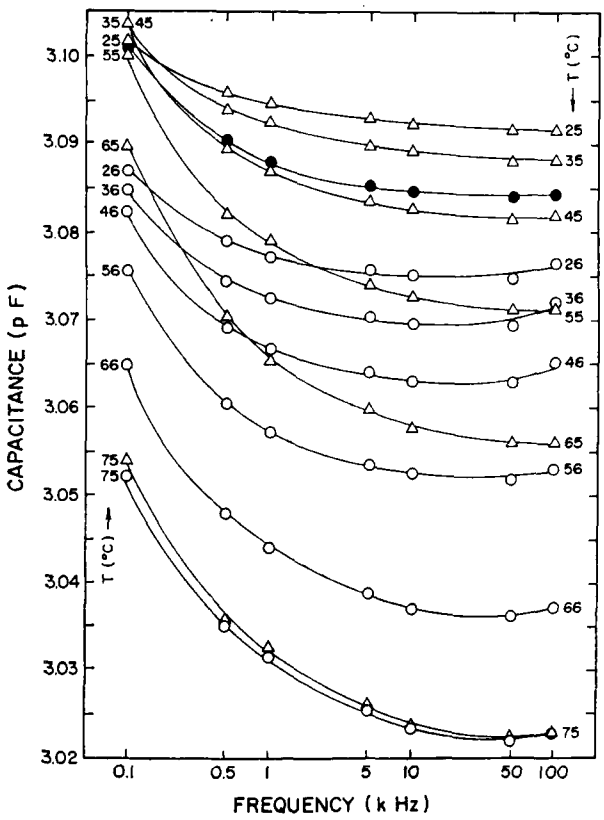

Figure 3. Dielectric capacitance versus excitation frequency at selected temperatures. △: heating, ○: cooling, and ●: 15-day recovery value.

3. Dilatometry

Single crystal dilatation studies of sufficient resolution for analyzing the preceding dielectric data have not been published previously. A capacitance type dilatometer was designed for examining small organic crystals. A description of this unit can be found elsewhere.[14] The essential features are shown in Fig. 4. The fused quartz substrates are held in a precision piston-and-cylinder arrangement which is incorporated into a sealed chamber. Electrical connectors come through small holes in the substrates to contact thin film electrodes in a guarded-field configuration. The

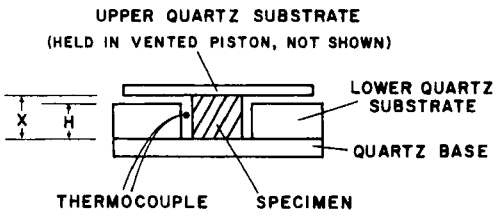

Figure 4. Capacitance dilatometer arrangement.

capacitance, as measured between the upper two quartz pieces, can be described by Eq. (1). Equation (2) is the rigorous expression for the expansivity, α, in terms of this geometry. It was found that, for expansivities much greater than that of fused quartz, the first two terms could be neglected and Eq. (2) can therefore be approximated by Eq. (3). The parameter k is evaluated for each specimen from initial conditions.

$$C = k/(X - H) \tag{1}$$

$$\alpha \equiv \left(\frac{1}{X}\frac{dX}{dT}\right) = \left(\frac{C}{k + CH}\right)\left(\frac{dH}{dT} + \frac{1}{C}\frac{dk}{dT} - \frac{k}{C^2}\frac{dC}{dT}\right) \tag{2}$$

$$\alpha \cong \frac{-k}{C(CH + k)}\frac{dC}{dT} \tag{3}$$

The a–b plane of a phenanthrene single crystal may be determined from cleavage properties. The a and b axes can subsequently be determined from the birefringent properties of the crystal.[15,16] Thus the a–c' and b–c' planes can also be determined. Various phenanthrene specimens with different orientations have been used in the capacitance dilatometer. The initial series of measurements in the c' direction was performed using discrete set-point temperatures. Anomalous peaks were observed in the thermal expansion coefficient. The succeeding series of measurements were performed on high purity specimens for the c', a and b directions, and included programmable continuous temperature changes. These changes were made through the transition region at rates from 1 to 8 °C/hour. A strip-chart recorder provided a continuous record of dilatometer capacitance and specimen temperature. Data were processed by digital computer methods and final results displayed on a CALCOMP Plotter (a computer directed drafting machine).

The same qualitative features were observed in the dilatation data for both c' series of measurements, with the peaks better resolved in the latter. Although different temperature rates were used in different sequences, most of the dilatation data were obtained with the 1 °C/hour rate employed at the end of each series of measurements to leave the specimens in an annealed condition.

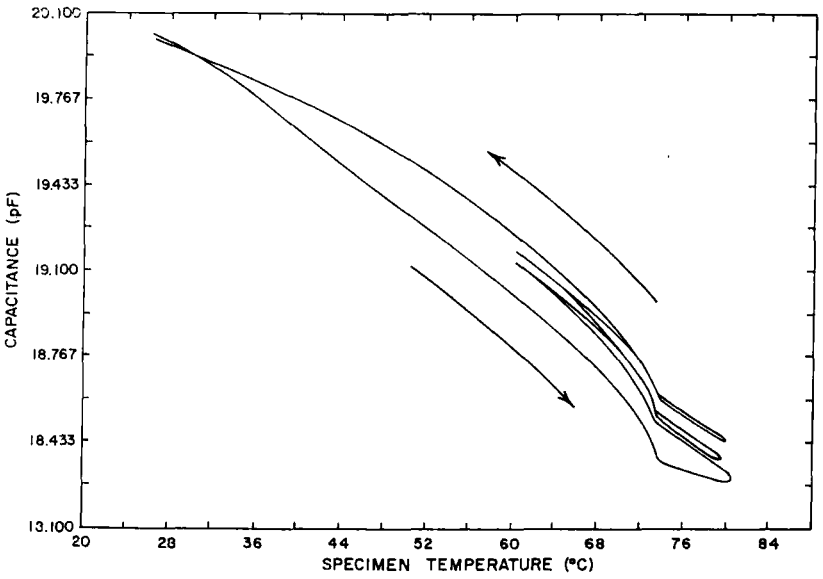

Figure 5. Dilatometer capacitance versus temperature for the c' direction. After the initial heating, the temperature is cycled several times across the transition region before the final cooling back to 26 °C.

Figure 5 shows the plot of dilatometer capacitance versus temperature for the continuous c' run. The fact that the final room temperature value of capacitance was nearly equal to the starting value indicates that the curve shifts were primarily due to a hysteresis type effect. Figure 6 shows expansivity computed from portions of the first two temperature curves of Fig. 5. Both were obtained at 4 °C/hour, but are representative of other rates; α, for c', peaks sharply around 73.3 °C for any heating rate up to 8 °C/hour on an annealed specimen, but shows evidence of quenching for cooling rates as low as 4 °C/hour. Similar behavior was observed for the a

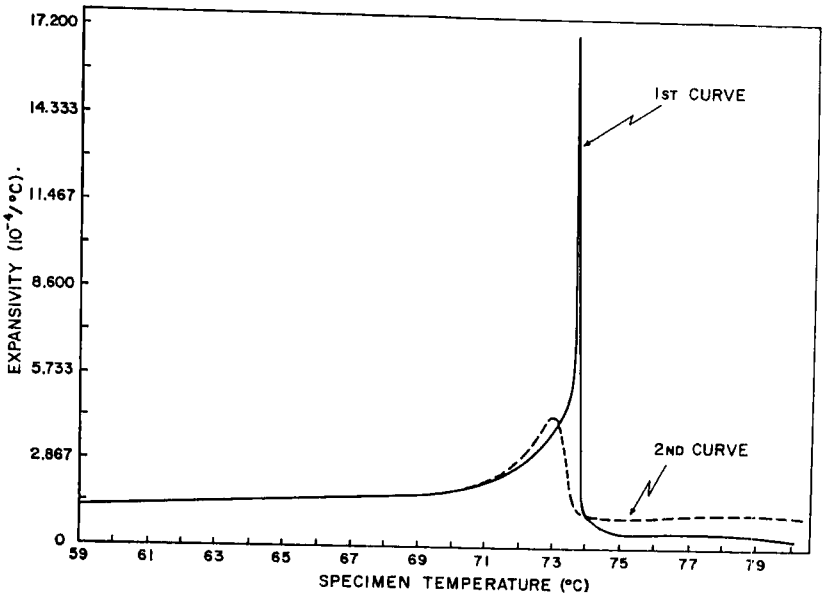

Figure 6. Measured expansivity for the c' direction using the first two curves of Fig. 5.

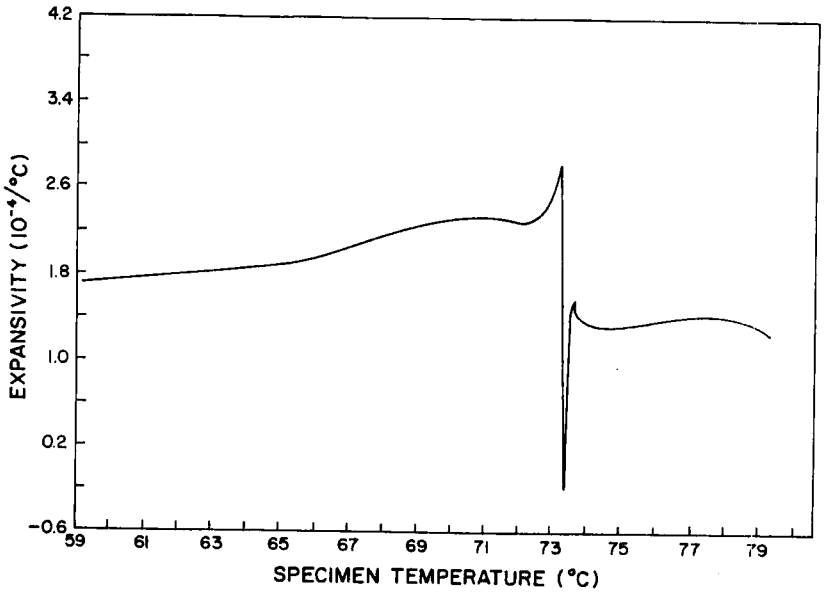

Figure 7. Measured expansivity for the b direction.

direction except that the α peaks were as high as 77.5 referred to the scale of Fig. 6.

The behavior of the expansivity along the direction of b is shown in Fig. 7. For this direction, α undergoes a sharp dip at the same temperature for which peaks were observed for the a and c' directions, namely at 73.3 °C.

Data were selected to be representative of the dilatometry results in the three orthogonal crystal directions. These were normalized to unity at room temperature and tables of interpolated values were generated so that a digital computer could be used to calculate products and ratios of these geometrical variations as functions of temperature. The resulting curves for a, b, and c' (as plotted directly by the computer) are shown in Fig. 8. The reciprocal of the c' variation in Fig. 8 is shown in Fig. 9. Figure 10 shows the type of behavior which would have been exhibited by the dielectric capacitance if it varied only with the ratio of the specimen area to thickness, i.e.: $(a \times b/c')$. The significance of Figs. 9 and 10 will become more apparent when the dielectric capacitance measurements are discussed in the next section.

Various possible sources of undesirable effects that could influence the dilatometry measurements were considered. The effect of piston weight was examined through use of several different pistons for the c' direction. Microcreep has not been proven to be totally absent, but has at least been shown not to be the major cause of the curve separations in Fig. 5. For the first two c' dilatometry specimens, temperature plateaus below and above the transition were monitored. These were at 64° and 79 °C for the first run and at 60° and 80 °C for the second. In each case, below the transition, capacitance drift could no longer be observed within a few minutes of stopping the temperature change. At the upper plateaus, measurement over periods ranging from $1\frac{1}{4}$ to 16 hours showed that the drift never vanished, but that it was slower at each successive temperature maximum and slightly slower using the lighter pistons. This suggests a " conditioning " of the specimen and, possibly, of the enclosed atmosphere.

The use of the electrode-piston assembly permits larger electrode areas (hence, higher sensitivity) than would a capacitance dilatometer with one electrode painted on the specimen. Also, the use of guard

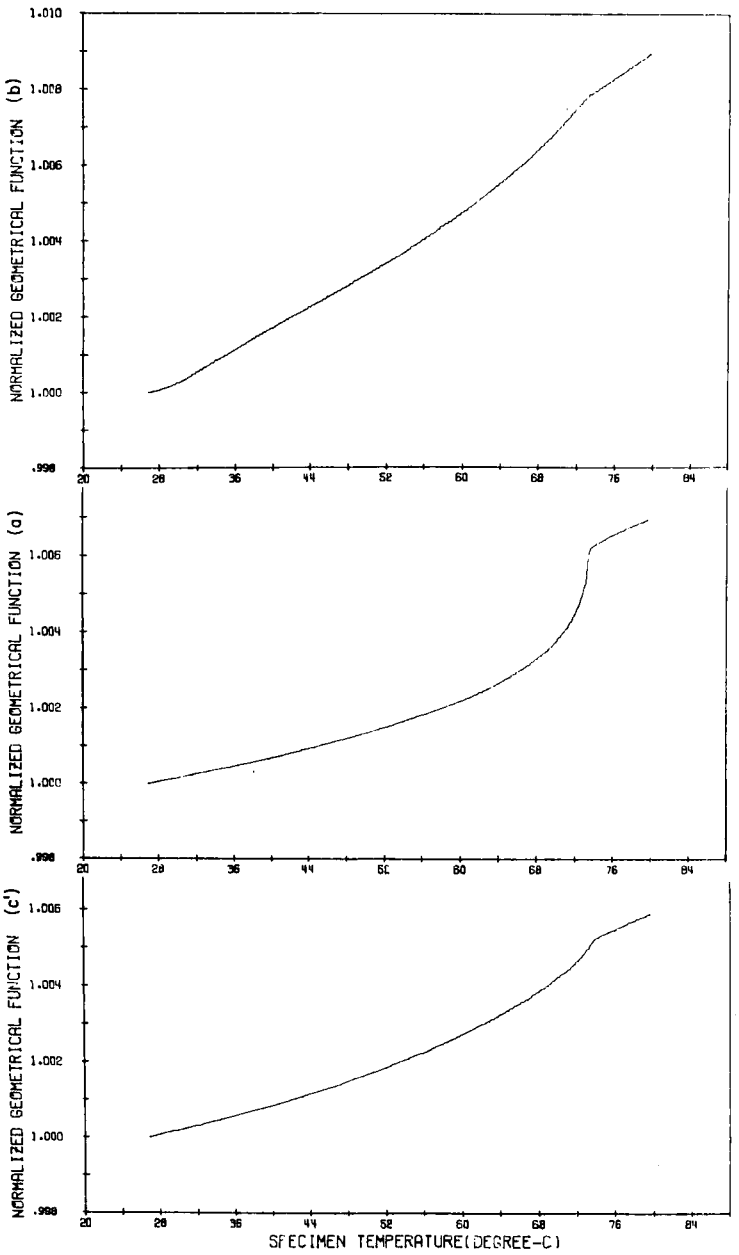

Figure 8. Normalized length as a function of temperature for the a, b and c' directions.

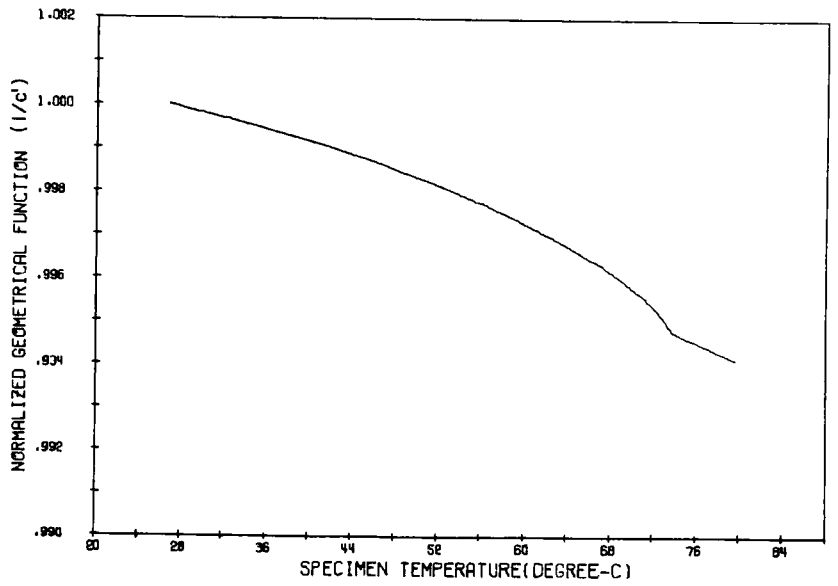

Figure 9. Normalized variation of reciprocal length, $(1/c')$, as a function of temperature for the c' direction.

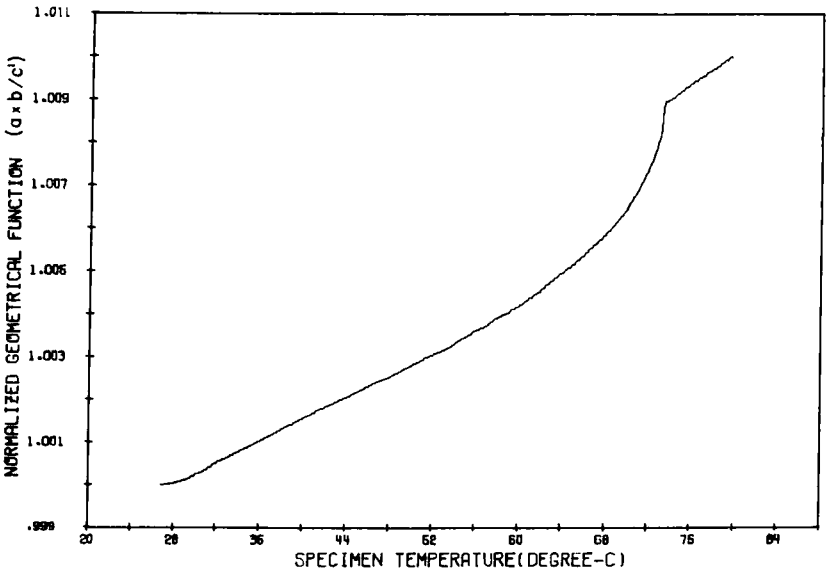

Figure 10. Data of Figs. 8 and 9 plotted to form the function $(a \times b/c')$.

rings in the piston electrodes eliminates the errors from fringing capacitance. It would appear, therefore, that the only way to completely eliminate possible microcreep errors due to the piston weight would be to have available considerably larger specimens so that adequate sensitivity could be obtained with one electrode painted on the specimen. This would require that the guarded electrode be stationary.

Fused quartz reference specimens were used at room temperature with air as the dielectric to verify Eq. (1). The measured calibration curve was parallel to, and shifted slightly down in magnitude, from the curve calculated with allowance for guard gap corrections. One of the quartz specimens was measured up to 100 °C, in air and with argon sealed at gauge pressures of 0 to 5 lb/in^2, both with and without chips of phenanthrene also in the chamber. For each calibration run the plot would appear as a horizontal straight line on the scale of any of the phenanthrene dilatometry plots. The effect of phenanthrene vapor subliming from the chips during the heating cycle was to cause a small but measurable change in the slope of the straight line calibration plot for the cooling cycle; this effect seemed to reach equilibrium with the first heating to maximum temperature. After cooling, vapor-deposited crystals could not be detected in the chamber upon microscopic examination. Also, for both calibration and data trials, measurement of the gauge pressure after each sequence showed no apparent loss of argon gas. The dilatometer was provided with effective mechanical vibration isolation. Tapping the dilatometer, at any temperature plateau during a trial with the quartz specimen, produced changes in the sixth significant digit of the capacitance bridge.

For the continuous phenanthrene dilatometry, small phenanthrene chips (of the same purity as the specimen) were distributed throughout the dilatometer to help establish the solid–vapor equilibrium. Even so, on the plots of dilatometer capacitance versus temperature, there is evidence of a possible increase in the dielectric constant of the dilatometer atmosphere, primarily with the first heating cycle. As the comparable effect had been small with the quartz specimen plus phenanthrene chips, and the maximum temperature employed for phenanthrene specimens was about 20 °C less than that for the quartz specimen trials, this effect is thought to be negligible for the

phenanthrene specimen measurements. It is therefore concluded that the expansivity behavior exhibited around 73.3 °C for the a, b, and c' directions of phenanthrene can be primarily attributed to the intrinsic behavior of single crystal material.

4. Discussion

A correlation was made of the dielectric and dilatometry results. Figures 9 and 10 show how the dielectric capacitance would vary with temperature if only dimensional changes were involved. The data of Fig. 2 suggest that the geometrical dependence of the dielectric capacitance varies as $1/c'$, rather than as $(a \times b/c')$. This was expected, since adhesion of the electrodes to the specimen implies that the number of specimen molecules between the electrodes does not vary with temperature. Thus, the electrode area can be treated as a constant for performing the differentiation in Eq. (6) below. The fact that the dielectric capacitance does not follow a curve of lesser slope above the transition temperatures, as does the $1/c'$ curve, suggests a variation in the permittivity itself. From an order of magnitude calculation, it can be demonstrated that it is reasonable to treat the edge capacitance of the specimen as constant. Thus,

$$C_{TOTAL} = C_E + C(\kappa_R, T) \tag{4}$$

and

$$C(\kappa_R, T) = \frac{\epsilon_0 A}{|c'(T_0)|} \frac{\kappa_R(T)}{L(T)} = C_V \frac{\kappa_R(T)}{L(T)}, \tag{5}$$

where: $L(T) \equiv |c'(T)|/|c'(T_0)|$ is the normalized length variation in the c' direction; T_0 is room temperature; and $\kappa_R(T)$ is the relative permittivity of the specimen. Define κ_0 by $\kappa_0 \equiv \kappa_R(T_0)$ so that $E(T)$ is defined by $E(T) \equiv \kappa_R(T)/\kappa_0$. Denoting the expansivity in the c' direction by α, and treating both the edge capacitance and electrode area as constants, it follows that

$$\frac{dC_{TOTAL}}{dT} \simeq \kappa_0 C_V \left\{ \frac{1}{L(T)} \frac{dE(T)}{dT} - \frac{\alpha E(T)}{[L(T)]^2} \right\}. \tag{6}$$

Rearranging gives

$$\frac{dE(T)}{dT} = \frac{L(T)}{\kappa_0 C_V} \frac{dC(\kappa_R, T)}{dT} + \frac{\alpha E(T)}{L(T)}. \tag{7}$$

Analysis by computer methods for $E(T)$, using Eq. (7) and iterating for stepwise increments in starting parameters, showed that the permittivity appears to increase on the order of 1% from room temperature to 75 °C. The starting parameters for which this 1% increase was found indicated a larger value of κ_R at room temperature (approximately 7) than the value determined from Table 1. This discrepancy can be attributed to the following factors: (a) a precise correction for the fringing capacitance could not be obtained from direct measurement or calculation. (b) It was not possible to measure κ_R and α on the same specimen. (c) Several series of computer calculations, involving three-point formulas for interpolation and approximation to derivatives, introduced numerical errors which were most pronounced around the transition region. It was found that values of the starting parameters κ_0 and C_V consistent with κ_R approximately equal to or less than 3, in the calculations of Eq. (7), caused the function $E(T)$ to nearly vanish by 75 °C and had to be discarded.

It has been shown that anomalous changes take place in the expansivity and dielectric permittivity of phenanthrene within a few degrees of 70 °C. These anomalies appear at very nearly the same temperature as do anomalies in heat capacity[7] and polarization.[8] Based upon the polarization data, a model has been proposed in terms of the molecular configuration changes at the anomaly temperature.[17] It is not entirely clear, however, that the effects observed in the present work can be explained by this model. For example X-ray data indicate a line splitting appropriate for a transformation between two monoclinic structures.[10] It is clear further work is required in order to relate the X-ray finding to present results as well as to any physical models. Some interesting extensions of the proposed model[17] were explored during the course of this investigation.[18]

It is evident from the present work that the transformation mechanism at the anomaly temperature is relatively slow. This is shown by the hysteresis at temperature changes as low as 1 °C per hour. A careful kinetic study is needed to determine the transformation mechanism. This study would be very difficult though because of the piezoelectric nature and poor thermal conductivity of phenanthrene. The effects of poor thermal conductivity are seen

in the variation of the critical temperature with heating or cooling rate; shifts of up to several degrees centigrade for rates on the order of 0.2 to 0.4 °C per minute were reported in resistivity measurements.[6] It is believed that major improvements on the dielectric and dilatometry results reported here must await the availability of significantly larger single crystal specimens of comparable or improved purity.

Acknowledgement

The authors gratefully acknowledge Brookhaven National Laboratory for providing the high purity samples used in this investigation, and one of us (D. A. M.) also expresses appreciation to BNL for the opportunity to visit and participate in the organic crystal group as a temporary research assistant.

REFERENCES

1. Andrews, P. A., Armington, A. F. and Rubin, B., *Appl. Phys. Letters* **7**, 86 (1965).
2. Peters, E. T., Armington, A. F. and Rubin, B., *J. Appl. Phys.* **37**, 226 (1966).
3. Matsumoto, S. and Tsukada, T., *Bull. Chem. Soc. Japan* **38**, 2023 (1965).
4. Matsumoto, S., *Bull. Chem. Soc. Japan* **39**, 1811 (1966).
5. Matsumoto, S. and Fukuda, T., *Bull. Chem. Soc. Japan* **40**, 743 (1967).
6. Matsumoto, S., Science Report Series I, Vol. LI (Tohoku Univ.), 133 (1968).
7. Arndt, R. A. and Damask, A. C., *J. Chem. Phys.* **45**, 755 (1966).
8. Arndt, R. A. and Damask, A. C., *J. Chem. Phys.* **45**, 4627 (1966).
9. Ringel, H., Damask, A. C. and Arndt, R. A., *Mol. Cryst.* **3**, 145 (1967).
10. Chiang, K., Forsyth, P., Morrison, L., Cohen, J. B. and Kauffman, J. W., *Phys. Letters* **30A**, 530 (1969).
11. Miller, D. A., Kauffman, J. W., Kannewurf, C. R. and Arndt, R. A., *Phys. Letters* **28A**, 75 (1968).
12. Meredith, C. C. and Wright, G. F., *Can. J. Chem.* **38**, 1177 (1960).
13. Murphey, E. J. and Morgan, S. O., *Bell System Tech. J.* **16**, 492 (1937).
14. Miller, D. A., Kauffman, J. W., Kannewurf, C. R. and Arndt, R. A., *Rev. Sci. Instr.* **42**, 155 (1971).
15. Nakada, I., *J. Phys. Soc. Japan* **17**, 113 (1962).
16. Gordon, R. B., *Acta. Met.* **13**, 199 (1965).
17. Damask, A. C., Arndt, R. A., Spielberg, D. H. and Lefkowitz, I., *Bull. Am. Phys. Soc.* **13**, 1394 (1968); *J. Chem. Phys.* **54**, 2597 (1971).
18. Miller, D. A., Ph.D. Thesis, Northwestern Univ., June (1970) (unpublished).